

# Capacitive Micromachined Ultrasonic Transducer Arrays For Medical Imaging: Experimental Results

U. Demirci\*, Ö. Oralkan, J. A. Johnson, A. S. Ergun, M. Karaman, B. T. Khuri-Yakub  
E. L. Ginzton Laboratory, Stanford University, Stanford, CA 94305-4085

**Abstract**—Capacitive micromachined ultrasonic transducer (cMUT) arrays provide broad bandwidth, high sensitivity, low mechanical impedance, and potential for electronic integration, and thus are promising for medical imaging applications. We have designed and fabricated 1D and 2D cMUT arrays of various sizes using standard integrated circuit fabrication processes. We improved the device parameters for medical imaging applications to achieve fully functional 64- and 128-element linear 1D cMUT arrays. We have also built a computer controlled experimental setup for collecting pulse-echo data from the test phantoms using cMUT arrays. In this paper the design and optimization of the immersion cMUTs for medical imaging system are discussed, and the phased array B-scan sector images taken by 1D cMUT arrays are presented.

## I. INTRODUCTION

Piezoelectric devices have been the primary transducer technology in medical ultrasonic imaging. In the last decade, cMUTs have emerged as an alternative to conventional piezoelectric transducers [1, 2]. The main benefit of cMUTs is that they have low self-noise, broad bandwidth and high sensitivity. [3]. In addition, they are easy to fabricate in 1D and 2D arrays using standard integrated circuit fabrication processes.

The first imaging results shown by using cMUTs were proof-of-concept experiments based on receiving from an active source placed at a distance in a tank of oil [4]. The first pulse-echo imaging using a 1D cMUT array was demonstrated in [5]. The array used in the first pulse-echo B-scan sector imaging had high collapse voltages around 50V, which caused problems in terms of switching with relays, and automated control of imaging. Only a 16-element portion of a 64-element array was used due to the problems in the process yield.

Recently, with improvements in our process flow to achieve 100% yield, we were able to fabricate fully functional 64- and 128-element immersion 1D cMUT arrays. We also built a computer-controlled automated experimental

setup to collect pulse-echo data. In this paper, we present the first pulse-echo B-scan sector images of a wire phantom obtained with 64 element 1D cMUT arrays.

## II. CMUT FABRICATION

A cMUT cell is basically a membrane suspended over a very highly doped silicon substrate. The topside of the membrane is coated with an electrode that creates a capacitance to the ground. In order to operate the cMUT, a DC voltage is applied to pull the membrane down close to the bottom electrode by the effect of the Coulomb attraction force. If an AC voltage is applied on top of the DC voltage, the membrane starts to vibrate and generates a pressure wave in the surrounding medium. On the other hand, when an ultrasound signal hits the surface of the DC biased membrane, a current is generated in the receiving circuitry due to the changing capacitance.

A 1D array is composed of 64 elements next to each other as seen in Figure 1. Each element has membranes connected in parallel as shown in Figure 2.

The fabrication process involves surface micromachining and is compatible with standard IC manufacturing technology. The processing starts with heavily doping a 4" n-type (100) silicon wafer with phosphorus. The purpose is to achieve good conductivity at the surface that forms the bottom electrode. Then, a thin layer of LPCVD SiN<sub>x</sub> is deposited as an etch stop in the sacrificial etching with KOH. Poly-silicon is deposited and patterned in order to form the sacrificial layer that defines the active area. A second layer of LPVCD SiN<sub>x</sub> is then deposited which later becomes the membrane. The critical point here is to achieve a low-tensile stress in the membrane. Etch holes are dry-etched to allow a path for the KOH to etch the sacrificial poly-silicon layer. The membranes are released, when the sacrificial layer is removed [8]. The vacuum

---

\* utkan@stanford.edu

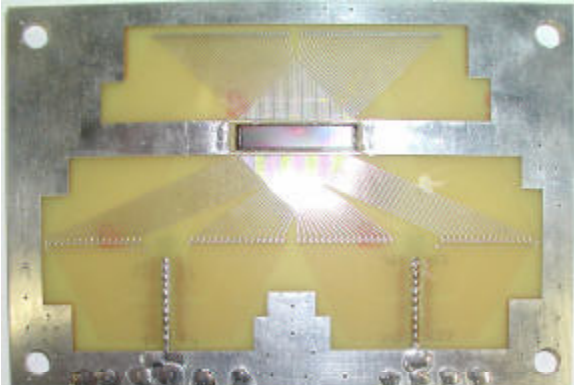


**Figure 1: 128-Element 1D cMUT array mounted on the fanout board.**

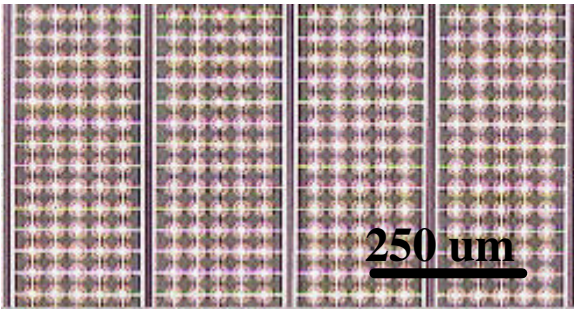


**Figure 2: 1-D array elements.**

sealing is done by additional  $\text{SiN}_x$  deposition. Finally, aluminum is sputtered and wet etch patterned to act as the top electrode.

### III. PROCESS IMPROVEMENTS

The transducer geometry is significant for the determination of the transducer characteristics. The process capabilities and device performance requirements determine the device dimensions. The sealing is required because the water fills in the gaps under the membrane and increases the loss for the immersion devices while the membrane is moving. The gap thickness is dependent on the sealing mechanism because the  $\text{SiN}_x$  has a very low sticking coefficient and 1/3 of the deposited  $\text{SiN}_x$  ends up under the membrane while sealing. To achieve a better control over the gap and membrane thickness, we separated the etch channel and active area definitions. In this way, we can make the etch channels as thin as possible independent of the gap thickness as shown in Fig. 3. This method has two advantages: the etch channels seal much faster, and very little  $\text{SiN}_x$  gets inside the gap. The other important aspect of this approach is that the array element still works even if some of the

membranes break, since all the membranes are isolated from each other.

In the previous process the gap thickness was initially chosen to be 3000 Å, and 6000 Å of  $\text{SiN}_x$  was necessary to seal the membranes. 2000 Å of  $\text{SiN}_x$  was getting deposited inside the gap decreasing the vacuum gap thickness to 1000 Å. In the recent process, the initial gap thickness was 1500 Å before sealing. The lowest channel height achieved is 500 Å using the new method. In this new process, 1000 Å of  $\text{SiN}_x$  are needed to seal the membranes. Only 300 Å of nitride goes under the membrane thus giving us a better control over the membrane and gap thickness.

Sealing increases the membrane thickness as much as the total deposited  $\text{SiN}_x$ . In order to bring the membrane back to the aimed design thickness, a dry etch back is used. This step was very critical due to the fact that over-etching of the membranes resulted in pinholes on the membrane surface causing malfunctioning devices. In the current process the membrane is deposited as thin as possible for most efficient operation and low DC bias. However, the membrane is still thick enough to avoid collapse, and to provide enough stress for successful release after sacrificial layer removal. The etch-back step is no longer necessary after the sealing.

The transducer metallization has two main functions: forming the circular metal plate at the top of the membrane, and interconnecting adjacent cells together. Smaller metallization area is always preferred due to lower parasitic capacitance.

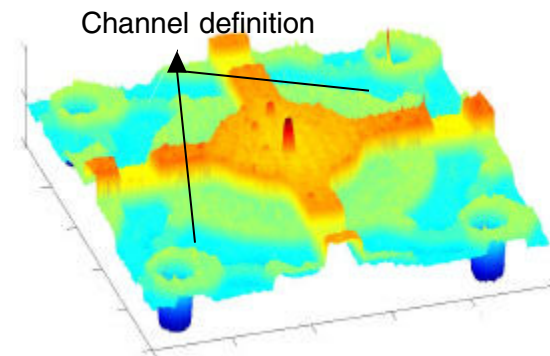


**Figure 3: Two step active area definition.**

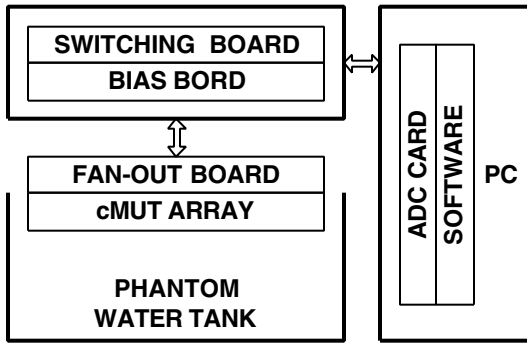


Figure 4: The experimental setup.

The design parameters are set according to a computer simulation that employs the equivalent circuit models explained in [6], [7]. The design parameters are a membrane radius of  $18\ \mu\text{m}$ , a gap thickness of  $0.12\ \mu\text{m}$ , a membrane thickness of  $0.88\ \mu\text{m}$ , and an insulator thickness of  $0.2\ \mu\text{m}$ . The device has a resonant frequency of 12 MHz in air. The element pitch is  $250\ \mu\text{m}$ , which is suitable for imaging at 3 MHz. Although the devices resonate at 12 MHz in air, the low mechanical impedance of the cMUTs is damped when immersed in water, yielding around 100% bandwidth.

#### IV. PULSE-ECHO IMAGING

The experimental setup is shown in Fig. 4. It includes a fan-out board for the cMUT array, a biasing board, and an RF board that has TX/RX switches, front-end amplifiers and multiplexers to reduce the number of channels that go to the A/D card installed on the controlling computer. The phantom consists of uniformly spaced, parallel stainless steel wires submerged in oil. The wires are arranged in a diagonal fashion in order to measure the point-spread functions at different spatial locations. The wire phantom and the cMUT array are immersed in oil. All the switching among the array elements is done by computer software.

A sample of the echo signals coming from the phantom wires is shown in Fig. 5. There are a total of 7 wires visible in the received echo signal. The applied signal is a unipolar pulse with a width of 100 ns width resulting in a broadband signal. Therefore, we can determine the two-way frequency response of our cMUT array elements by looking at the Fourier Transform one of the echo signals. A sample echo signal and its Fou-

rier Transform are shown in Figs. 6 and 7, respectively. Figure 7 shows that the overall re-

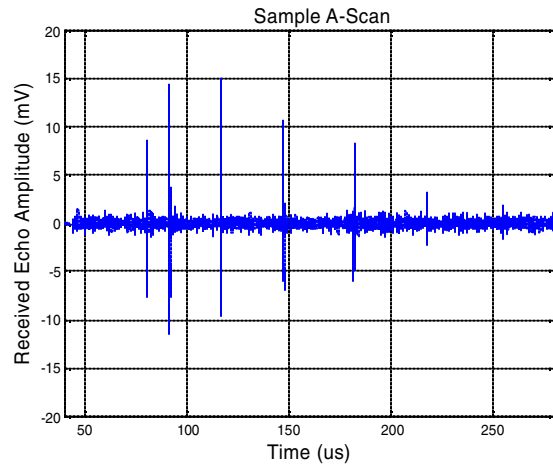


Figure 5: A Sample A-scan acquired from the wire phantom.

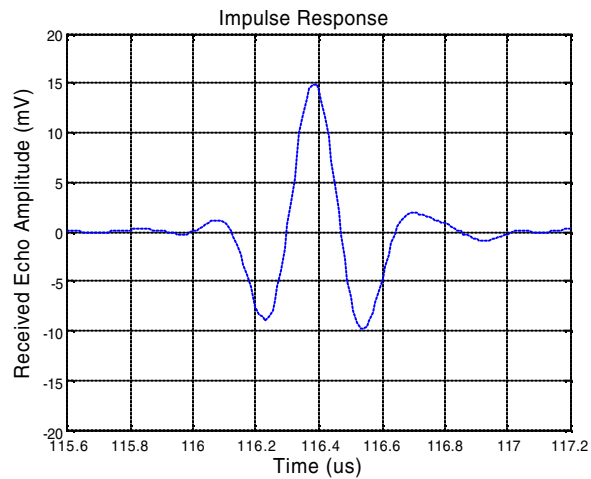


Figure 6: Pulse-echo Impulse response of the cMUT array element.

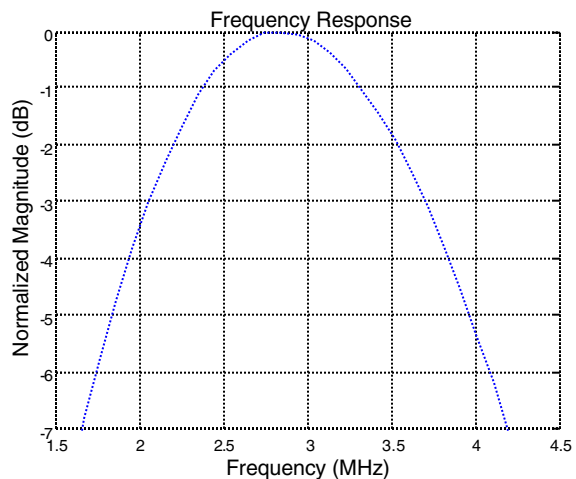


Figure 7: Pulse-echo Frequency response of the cMUT array element.

sponse has a fractional bandwidth of 85%, a promising result for medical imaging. However, the actual bandwidth of the cMUT is even larger. Taking the diffraction and medium losses



**Figure 8: B-scan sector image using 64 element 1D cMUT array. Display dynamic range is 50 dB.**

into account, the fractional bandwidth increases to more than 100%.

The image is reconstructed by employing RF beamforming and synthetic phased array approaches [9]. Dynamic focusing is employed in transmit and receive beamforming. The resulting B-scan sector image is shown in Fig. 8. The display dynamic range is 50 dB.

## V. CONCLUSIONS

We demonstrated the successful operation of immersion cMUT arrays operating at around 3MHz, an operating point suitable for medical imaging. The modifications in the process enable the fabrication of fully functional 1D and 2D arrays. These arrays are then used in our experimental setup to image wire phantoms. The broad bandwidth and high sensitivity of the cMUTs are confirmed through improved axial and lateral resolution depicted by the experimental imaging results. The grating lobe artifact is observed at 90 degree angle off the first reflector. The inter-element spacing of the array is 250  $\mu\text{m}$ . This spacing satisfies the spatial sampling criteria for frequency components up to 3 MHz. Since the cMUT array element has broadband response, frequency components higher than 3 MHz cause the grating lobe artifact mentioned above. This is not a problem for narrow band for transducers. However, cMUT arrays should be designed so that the spatial

sampling criteria is not violated for the highest frequency components in the transducer response. Crosstalk between the array elements is observed which is due to Lamb waves propagating in the silicon wafer, and Stonley waves propagating at the fluid-silicon interface. The effects of cross-talk are not evident in the presented imaging results since imaging in the near field—the region most often affected by cross-talk—was not performed. Currently, reducing the crosstalk between the array elements by re-evaluating the fabrication and design is subject to extensive research in the future.

## VI. REFERENCES

- [1] M. I. Haller and B. T. Khuri-Yakub, "A surface micromachined micromachined Electrostatic electrostatic Ultrasonic ultrasonic Air air transducer," *IEEE Trans. on UFFC* 43, 1-6 (January 1996).
- [2] G. S. Kino, *Acoustic Waves*. Englewood Cliffs, NJ: Prentice-Hall, 1987
- [3] X. C. Jin, S. Calmes, C. H. Cheng, F. L. Degertekin, and B. T. Khuri-Yakub, "Micromachined capacitive ultrasonic immersion transducer array," in *Transducers'99*, Sendai, Japan, 1999
- [4] X. C. Jin, F. L. Degertekin, S. Calmes, X. J. Zhang, I. Ladabaum, and B. T. Khuri-Yakub, "Micromachined Capacitive Transducer Arrays for Medical Ultrasound Imaging," *Proceedings of IEEE Ultrasonics Symposium*, Sendai, Japan, 1998, pp. 1877-1880.
- [5] O. Oralkan, X. C. Jin, K. Kaviani, A. S. Ergun, F. L. Degertekin, M. Karaman, and B. T. Khuri-Yakub, "Initial Pulse-Echo Imaging Results with One-dimensional Capacitive Micromachined Ultrasonic Transducer Arrays," *Proceedings of IEEE Ultrasonics Symposium*, San Juan, Puerto Rico, 2000, pp. 959-962.
- [6] I. Ladabaum, X. C. Jin, H. T. Soh, F. Pierre, A. Atalar, B. T. Khuri-Yakub, "Micromachined ultrasonic transducers : Toward robust models and immersion devices," in *Ultrasonic Symposium*, San Antonio, Texas, 1996, pp. 335-338
- [7] W. P. Mason, *Electromechanical Transducers and wave filters*. New York: Van Nostrand, 1942
- [8] R. M. White, R. J. Wicher, S. W. Wenzel, and E. T. Zellers "Plate mode ultrasonic oscillator sensors" *IEEE Trans. Ult. Ferr. Freq. Control*, vol.34, no.2, pp. 162-171, 1987
- [9] M. Karaman, P. -C. Li, M. O'Donnell, "Synthetic aperture imaging for small scale systems," *IEEE Trans. on Ultrason., Ferroelect., Freq. Contr.*, vol. 42, no. 3, pp 429-422, May 1995